Halide Anion Capture and Recognition by a Tetrahedral Tetraammonium Receptor in Water: A Molecular Dynamics Investigation

Alain Chaumont, Etienne Engler, and Georges Wipff*[a]

Abstract: We report molecular dynamics potential of mean force (PMF) simulations on the capture of halide anions X^- (F^-, Cl^-, Br^-) by a tetrahedral receptor $\mathbf{L}^{4+}$ built from four quaternary ammonium sites connected by six $(CH_2)_n$ chains, leading to the formation of inclusion complexes $X^- \subset \mathbf{L}^{4+}$. Simulations performed with a reaction field correction of the electrostatics and with PME-Ewald summation gave very similar energy profiles. In aqueous solution, an energy barrier of 12-17 kcal mol^{-1} was found for the three anions, mainly due to their dehydration when they enter through the largest triangular face of $\mathbf{L}^{4+}$. In the inclusion complexes, the anion is anchored near the center of the cavity due to the electrostatic field of the four positively charged ammonium sites, shielded from the surrounding water molecules. It was predicted that $\mathbf{L}^{4+}$ is selective for Cl^- over Br^- which both form stable inclusion complexes, while the F^- complex should dissociate. The comparison of PMFs in aqueous solution and in the gas phase and the energy component analysis demonstrates the importance of solvent on the nature of these complexes and on the complexation energy profiles. The Cl^-/Br^- selectivity obtained from the dissociation pathways in water was in good agreement with the results of free energy perturbation simulations based on the "alchemical route" of a thermodynamic cycle, and consistent with experimental observations.

Keywords: anions · macrocyclic chemistry · molecular dynamics · molecular recognition

Introduction

Anion X^- complexation by macro(poly)cyclic hosts is generally achieved through hydrogen bonding interactions with polar bonds (e.g. $N^{\delta-}H^{\delta+}\cdots X^-$), or with Lewis acids.[1–7] Quaternary ammonium sites cannot form such bonds, but in suitable organized arrangements, their +1 charge may cooperatively contribute to a strong positive electrostatic potential suitable for anion complexation, as elegantly demonstrated by Schmidtchen who developed tetrahedral receptors possessing four N^+ sites connected by $(CH_2)_n$ chains "C_n" (Figure 1).[8] In aqueous solution, the largest cage (six C_8 chains and four N^+-CH_3 corners) displays a selectivity order $Cl^- < Br^- < I^-$, while with a smaller cage (six C_6 chains), the order is $Cl^- < I^- < Br^-$.[9] The present paper deals with a smaller analogue (hereafter noted $\mathbf{L}^{4+}$; see Figure 1) synthetized by Ichikawa et al.[10] The tetrahedron delineated by the four nitrogen bridgeheads is not regular, as $\mathbf{L}^{4+}$ is built from three C_5 and three C_6 chains. The C_6 chains intersect with the C_3 pseudo-symmetry axis, which is perpendicular to a small [5,5,5] triangular face delineated by three C_5 chains. To our knowledge, no stability constants have been reported for this host, but an X-ray structure indicates that Cl^- nicely fits inside the cavity of $\mathbf{L}^{4+}$;[10] in an acetonitrile solution, $\mathbf{L}^{4+}$ prefers Cl^- over Br^-.[11] Ordered arrays of chloride complexes of $\mathbf{L}^{4+}$ have also been characterized at the interface between a NaCl surface and water.[12] Tetrahedral analogues of $\mathbf{L}^{4+}$ with

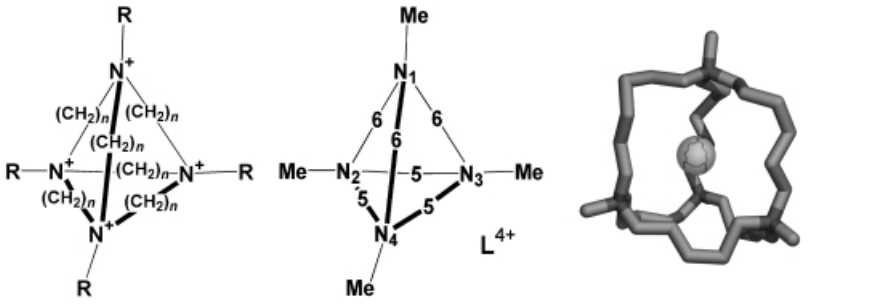

Figure 1. Schematic representation of tetrahedral tetraammonium hosts, of $\mathbf{L}^{4+}$ and X-ray structure of its $Cl^- \subset \mathbf{L}^{4+}$ complex. The numbers 5 and 6 along the edges of the tetrahedron correspond to $(CH_2)_5$ and $(CH_2)_6$ chains, respectively.

[a] Prof. G. Wipff, A. Chaumont, E. Engler
Laboratoire MSM, Institut de Chimie
4 rue B. Pascal, 67000 Strasbourg (France)
Fax: (+33) 3 90 24 15 45
E-mail: wipff@chimie.u-strasbg.fr

  0947-6539/03/0903-0635 $ 20.00+.50/0

different (*m*,*n*) combinations of $m\,C_5$ and $n\,C_6$ bridges have also been studied experimentally; this shows how tailoring the cavity size allows to monitor the anion selectivity. For instance, the (*4*,*2*) host also binds selectively Cl^-,[11] while the smaller (*6*,*0*) one prefers F^-.[12] The larger (*2*,*4*) and (*0*,*6*) hosts prefer Br^-[13] and I^-,[14] respectively.

Our aim is to calculate the free energy profile for the capture of halide anions X^- by $\mathbf{L}^{4+}$, leading to the inclusion complexes (noted $X^- \subset \mathbf{L}^{4+}$). As solvent we chose water, because water strongly competes with the complexation process (the dehydration free energies of F^-, Cl^- and Br^- are 112.9, 83.0, and 76.8 kcal mol^{-1}, respectively[15]) and it is important to determine to which extent the host–guest interactions will be strong enough to compete with these solvation forces and to examine the driving forces for anion encapsulation and the basis of anion selectivity by $\mathbf{L}^{4+}$. In order to gain insights into the effect of solvent, the free energy profiles were also calculated in the gas phase, for comparison. The anion binding selectivity in water is also examined using the "alchemical transformation" based on the thermodynamic cycle approach.[16]

Methods

Representation of the potential energy of the system: The simulations were performed with the modified AMBER5.1 software[17] with the following representation of the potential energy:

$$U = \sum_{\text{bonds}} K_r (r - r_{eq})^2 + \sum_{\text{angles}} K_\theta (\theta - \theta_{eq})^2 + \sum_{\text{dihedrals}} \sum_{n} V_n (1+\cos n\phi) + \sum_{i<j} \left(\frac{q_i q_j}{R_{ij}} - 2\varepsilon_{ij} \left(\frac{R^*_{ij}}{R_{ij}} \right)^6 + \varepsilon_{ij} \left(\frac{R^*_{ij}}{R_{ij}} \right)^{12} \right)$$

The non-bonded interactions are represented by pairwise additive contributions of coulombic and van der Waals type which display a 1-6-12 dependence of the interatomic distances R_{ij}. The aqueous solvent was represented explicitly, using the TIP3P model.[18] The ESP charges on $\mathbf{L}^{4+}$ were derived from ab initio 6-31G* electrostatic potentials on diammonium constitutive fragments $Me_3N(CH_2)_nNMe_3^{2+}$ with $n = 5$ and 6. They are given in Figure 2 together with the AMBER atom types used for $\mathbf{L}^{4+}$. The 1-4 non-bonded interactions within the cage were calculated without scaling factor. The van der Waals parameters for F^-, Cl^- and Br^- ($R^*_F = 1.850$, $R^*_{Cl} = 2.495$, $R^*_{Br} = 2.679$ Å and $\varepsilon_F = 0.200$, $\varepsilon_{Cl} = 0.107$, $\varepsilon_{Br} = 0.0858$ kcal mol^{-1}) are those fitted by Berny et al. from free energy calculations of their hydration energies,[19] starting from the Cl^- values.[20] We performed ab initio optimizations of the $Cl^- \subset \mathbf{L}^{4+}$ inclusive complex with the 6-31G* basis set at the HF and DFT level. The corresponding BSSE corrected interaction energies between Cl^- and the host are -271.4 and -276.0 kcal mol^{-1}, very close to the value obtained by molecular mechanics minimization (-275.3 kcal mol^{-1}). Two protocols were used to calculate the non-bonded interactions, which will be noted in short 15 + RF and 13-PME, respectively. The first one uses an atom-based cut-off of 15 Å with a reaction field correction to the coulombic interactions.[21] This correction assumes that the charge distribution within the sphere of cut-off radius interacts with the polarizable dielectric medium represented by a continuum and corrects for discontinuities of the potential energy at the cut-off boundaries. The second procedure used a 13 Å cut-off and the PME-Ewald treatment of long range electrostatics, as used to describe long range electrostatic interactions in ionic crystals.

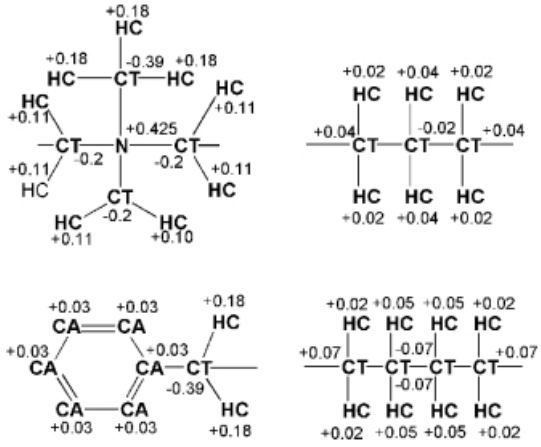

Figure 2. Atom types and atomic charges used on the constitutive fragments of $\mathbf{L}^{4+}$ and its derivatives.

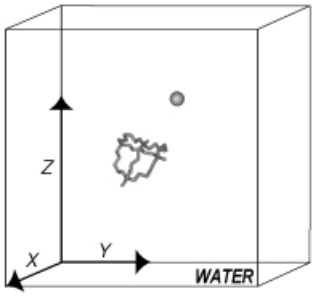

Figure 3. Schematic representation of the water box with a dissociated $X^- \cdots \mathbf{L}^{4+}$ complex.

Molecular dynamics: The MD simulations were performed at 300 K, starting with random velocities. The temperature was monitored by separately coupling the water, the complex and the *exo* anion subsystems to independent thermal baths using the Berendsen algorithm[22] with a relaxation time of 0.2 ps. All O-H, C-H and H···H "bonds" were constrained with SHAKE, using the Verlet leapfrog algorithm with a time step of 2 fs for the integration of the equations of motion. Equilibration started with 1000 steps of energy minimization, followed by 50 ps of MD with fixed solutes ("BELLY" option of AMBER) at constant volume (NVT ensemble), and by subsequent MD run of 25 ps at constant volume followed by 25 ps at a constant pressure of 1 atm without constraints.

0947-6539/03/0903-0636 $ 20.00+.50/0 *Chem. Eur. J.* **2003**, *9*, No. 3

Potential of mean force calculations: We calculated the potential of mean force (PMF)[23, 24] corresponding to the free energy profile for anion dissociation as a function of its position, which was varied stepwise from the state C (complex $X^- \subset \mathbf{L}^{4+}$) to the state UC (uncomplexed $X^- \cdots \mathbf{L}^{4+}$ system). As reaction coordinate, we used the $N \cdots X^-$ distance d (see Figure 4) between X^- and the nitrogen bridgehead which is opposite to the largest face [6,6,5], delineated by one C_5 and two C_6 chains. $\mathbf{L}^{4+}$ possesses three such faces, and we assume that passing through the [6,6,5] "gate" is easier than through the smallest [5,5,5] "gate". The d distance was increased linearly as a function of a λ parameter from d_c (complexed state C; $\lambda = 1$) to $d_{uc} = d_c + 10$ Å (uncomplexed state UC; $\lambda = 0$): $d_\lambda = \lambda d_c + (1-\lambda) d_{uc}$. For a given complex, d_c is obtained from the last set of MD equilibration (4–4.5 Å).

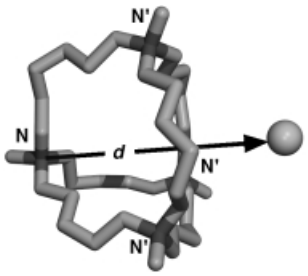

Figure 4. Definition of the "reaction coordinate" used to monitor the decomplexation of X^-.

The change in free energy between states defined by λ_1 and λ_2 was calculated at each step using the statistical perturbation theory with the thermodynamic integration TI technique based on Equation (1):

$$\Delta G = \int_{\lambda_1}^{\lambda_2} \left\langle \frac{\partial U}{\partial \lambda} \right\rangle_\lambda d\lambda \qquad (1)$$

The transformation of states C to UC was achieved in 51 steps, that is with increments $\Delta\lambda$ of 0.02, corresponding to 0.2 Å each. At each λ, we performed 10 ps of equilibration followed by 10 ps of data collection, and the changes of free energy ΔG were averaged from the forward and backward cumulated values.

Tests were also performed in the gas phase and in solution using the free energy perturbation method FEP, based on Equation (2) and similar conditions for equilibration and data collection.

Relative binding affinities in solution: The change in free energy when the X^- anion is stepwise mutated into Y^- in solution was calculated using the statistical perturbation FEP theory and the windowing technique,[23, 24] with

$$\Delta G = \Sigma \Delta G_\lambda \quad \text{and} \quad \Delta G_\lambda = RT \log \langle \exp(U_\lambda - U_{\lambda+\Delta_\lambda})/RT \rangle_\lambda \qquad (2)$$

The potential energy $U(\lambda)$ was calculated for the "hybrid anion" defined by a linear combination of R^* and ε parameters of the initial ($\lambda = 1$) and final state ($\lambda = 0$):

$$R_\lambda^* = \lambda R_1^* + (1-\lambda) R_0^* \quad \text{and} \quad \varepsilon_\lambda = \lambda \varepsilon_1 + (1-\lambda) \varepsilon_0$$

The mutation was achieved in 21 windows (of 2+3 ps each) and the changes in free energy ΔG_λ were averaged from the forward and backward cumulated values. Tests with 51 windows confirmed that the sampling obtained by 21 windows is sufficient, as the host is topologically constrained and changes in ΔG are quasi proportional to λ.

Energy and structural analysis of the simulated systems: The potential energy was analyzed at selected points along the trajectories in terms of the pairwise additive contributions of the solute/water ($U_{s/w}$), host/guest ($U_{L/X}$) interaction energies, and of the deformation energy of the host ΔU_L, defined as the energy difference between $\mathbf{L}^{4+}$ uncomplexed and $\mathbf{L}^{4+}$ within the system. The $U_{s/w}$ energy can be further dissected into the interactions of X^- and of $\mathbf{L}^{4+}$ with water: $U_{s/w} = U_{X/w} + U_{L/w}$. Interaction energies can also be split into their van der Waals and electrostatic components. The structural deformations of the host are characterized by the ρ ratio $\rho = S/\langle NN' \rangle$, where S is the surface of the "gating face" [6,6,5] delineated by one C_5 and the two C_6 chains, and $\langle NN' \rangle$ is the average distance between the three N-N′ distances (see Figure 4 for definition). A small ρ value corresponds to an "elongated" shape of $\mathbf{L}^{4+}$, while a large value corresponds to a flattened tetrahedron. ρ values of 3.08 and 3.06 are obtained from MD simulations of $\mathbf{L}^{4+}$ uncomplexed and for its $Cl^- \subset \mathbf{L}^{4+}$ inclusive complex in water, which compare well to the value of 3.07 Å for the X-ray structure of this complex.

Results

We first briefly describe the structure and solvation of the $X^- \subset \mathbf{L}^{4+}$ inclusive complexes in water. This is followed by the free energy profiles for anion decomplexation from $\mathbf{L}^{4+}$ in solution and in the gas phase and a comparison of Cl^- versus Br^- complexation through a thermodynamic cycle. Unless otherwise specified, all results are obtained with the 15+RF protocol.

Inclusive complexes $X^- \subset \mathbf{L}^{4+}$ in aqueous solution: The inclusive $X^- \subset \mathbf{L}^{4+}$ complexes were simulated in water for 0.5 ns in the presence of three neutralizing Cl^- counterions. The complexed Cl^- and Br^- anions remained encapsulated for the whole simulation, while F^- was captured by water in about 0.12 ns; this indicates that this anion is too small for $\mathbf{L}^{4+}$ and not shielded enough by this host to prevent its decomplexation.

As the tetrahedron formed by the four N^+ bridgeheads of $\mathbf{L}^{4+}$ is not regular, the Cl^- and Br^- anions sit slightly off the center of the cavity (at 0.5 ± 0.1 Å). They are not equidistant from the four nitrogen bridgeheads either, one distance being 0.4 to 0.5 Å shorter than the three others (Table 1). From Cl^- to Br^-, these distances also increase (by less than 0.1 Å on the average), but less then do the ionic radii (the difference in R* parameters is 0.18 Å, while their difference in ionic radii is 0.15 Å[19]), which is indicative of steric compression with the Br^- anion. According to the energy component analysis, the host/anion interaction energies $U_{L/X}$ are somewhat weaker (by

  0947-6539/03/0903-0637 $ 20.00+.50/0

Table 1. The $X^- \subset \mathbf{L}^{4+}$ inclusive complexes in water: average distances between X^- and the nitrogen bridgeheads and between X^- and the center of the cage.

	Distances				
	N_1^+	N_2^+	N_3^+	N_4^+	center
F^-	3.8 ± 0.1	4.3 ± 0.1	4.3 ± 0.1	4.4 ± 0.2	0.4 ± 0.1
Cl^-	3.9 ± 0.1	4.4 ± 0.1	4.4 ± 0.1	4.4 ± 0.1	0.4 ± 0.1
Br^-	3.9 ± 0.1	4.5 ± 0.1	4.5 ± 0.1	4.5 ± 0.1	0.5 ± 0.1

7 kcal mol^{-1}) with Br^- than Cl^-, mostly due to the van der-Waals contribution.

It is interesting to compare the interaction energies $U_{x/w}$ of the free anion with water and $U_{L/X}$ of the complexed anion with the host. For instance, with the Cl^- anion, average values over the last 0.2 ns are -128 and -277 ± 2 kcal mol^{-1}, respectively, showing the importance of host–guest interactions as a driving force for anion encapsulation. The entropy gain resulting from stripping the first hydration shell of the anion should also favor its complexation.

The shielding of encapsulated Cl^- or Br^- anions from water is well illustrated by the anion-water RDFs (Figure 5) which display no clear peak in the first shell.[25] Thus, the water structure around the complex is mostly determined by the hydrophobic nature and +4 charge of $\mathbf{L}^{4+}$, rather than by the complexed anion. This is also consistent with the energy component analysis, according to which the attraction energies of the $X^- \subset \mathbf{L}^{4+}$ complexes with water (-296 and -314 kcal mol^{-1} with Cl^- and Br^-, respectively) are due to the contribution of $\mathbf{L}^{4+}$ (-370 and -380 kcal mol^{-1}, respectively), while the contributions of X^- are repulsive (73 and 65 kcal mol^{-1}, respectively). In the case of F^- "complex", analysis prior decomplexation shows that the anion sits on one face of the host, and is hydrogen bonded to water molecules which pull it out.

Dissociation of F^-, Cl^-, Br^- anion complexes of L^{4+} in water and in the gas phase. Free energy profiles and energy component analysis: We simulated the stepwise dissociation of the three halide complexes in water. According to the microreversibility principle, dissociation and formation of the complex should follow the same pathways and display the same free energy profiles $\Delta G(d)$. We thus decided to simulate the dissociation only, in order to reduce the computational cost related to the conformational sampling of the uncomplexed states. The PMFs obtained for the three anions in water using the 15+RF and 13-PME protocols are shown in Figure 6 and the most important characteristics are given in Table 2. We also report in Table 3 the results of energy components analysis in terms of the interactions of groups

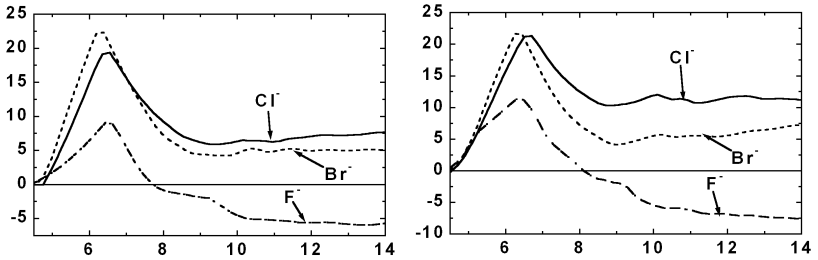

Figure 6. Calculated free energy profiles for the dissociation of $X^- \subset \mathbf{L}^{4+}$complexes in water, using the 15+RF (left) and 13-PME (right) protocols.

Table 2. Main energy characteristics [kcal mol^{-1}] of the PMFs in water: 15+RF and 13-PME results.

	C		TS		UC	
	15+RF	13-PME	15+RF	13-PME	15+RF	13-PME
F^-	0	0	9.1	11.3	−5.7	−7.6
Cl^-	0	0	19.4	21.4	7.8	11.2
Br^-	0	0	22.4	23.2	5.2	6.5

Table 3. Average energy component analysis for the complexed(C), transition state (TS) and uncomplexed (UC) states along the PMF (15+RF protocol) for anion decomplexation: host/guest interaction energy $E_{L/X}$, interactions of water with the complex ("solute" s) $U_{s/w}$, with the host $U_{L/w}$ and with the anion $U_{X/w}$ [kcal mol^{-1}]. Averages over 100 configurations (10 ps).

		C	TS	UC
$U_{L/X}$	F^-	−295 ± 3	−278 ± 4	−90 ± 3
	Cl^-	−277 ± 2	−260 ± 6	−100 ± 3
	Br^-	−270 ± 2	−242 ± 3	−120 ± 3
$U_{X/w}$	F^-	70 ± 6	43 ± 6	−180 ± 10
	Cl^-	73 ± 8	69 ± 6	−128 ± 8
	Br^-	65 ± 9	23 ± 10	−99 ± 8
$U_{L/w}$	F^-	−375 ± 21	−343 ± 26	−585 ± 24
	Cl^-	−370 ± 26	−438 ± 25	−492 ± 22
	Br^-	−380 ± 30	−367 ± 24	−550 ± 24
$U_{s/w}$	F^-	−306 ± 17	−300 ± 22	−766 ± 26
	Cl^-	−296 ± 22	−370 ± 20	−620 ± 24
	Br^-	−314 ± 29	−344 ± 20	−647 ± 24

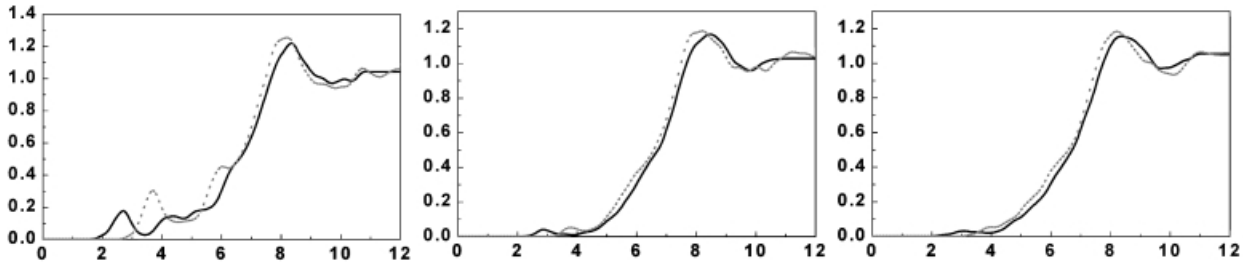

Figure 5. Radial distribution functions $X^- \cdots H_{water}$ (full line) and $X^- \cdots O_{water}$ (dotted line) for the inclusive $X^- \subset \mathbf{L}^{4+}$ complexes in water. The analysis with F^- corresponds to the first 100 ps, that is prior to decomplexation. From left to right: F^-, Cl^- and Br^- complexes.

0947-6539/03/0903-0638 $ 20.00+.50/0 *Chem. Eur. J.* **2003**, *9*, No. 3

(host, anion, solvent) at typical stages of anion decomplexation. A graphical presentation of the van der Waals and electrostatic components as a function of d is given in Figure 7 and typical structures of the "complex" are given in Figure 8. It can be seen from Figure 6 that the 15+RF and 13-PME protocols lead to similar energy profiles $\Delta G(d)$. This is why in the following, we discuss the 15 + RF results only for simplicity.

All $\Delta G(d)$ energies are given with respect to the inclusive complexes. With our definition of the reaction coordinate d, the anion exits the cage through the largest triangular face of the host ("gating face" of [6,6,5] type), which should be less energy demanding than passing through the smaller [5,5,5] face. A significant energy barrier is observed for the three anions in water, and this barrier is higher for the Cl^- and Br^- anions (19.4 and 22.4 kcal mol^{-1}, respectively) than for F^- (9.1 kcal mol^{-1}), following trends noticed above for the kinetic stability of these complexes. This barrier corresponds to d distances of 6.4, 6.2 and 6.6 Å, respectively, that is to a facial position of the anion which interacts mostly with the three nearest ammonium centers (Figure 8). Its corresponding interaction energy $U_{X/L}$ with $\mathbf{L}^{4+}$ ranges from -278 (F^-) to -242 kcal mol^{-1} (with Br^-), which indicates a decrease of about 5% only, compared with the inclusive $X^- \subset \mathbf{L}^{4+}$ complexes. At the "transition state" TS, the anion still displays repulsive interactions with water (23 to 70 kcal mol^{-1}), and is therefore not hydrated. At the TS, the deformation energies of $\mathbf{L}^{4+}$ relative to the $\mathbf{L}^{4+}$ inclusive complex are 7, 6 and 10 kcal mol^{-1}, for F^-, Cl^- and Br^-, respectively.

As the d distance is increased beyond the transition state, the energy $\Delta G(d)$ decreases and reaches a plateau at $\leqq$ about 13 Å. The corresponding energy drop amounts to 14.8 kcal mol^{-1} for F^-, 11.6 kcal mol^{-1} for Cl^- and 17.2 kcal mol^{-1} for Br^- at the end of the PMF. It thus does not simply follow the order of anion hydration energies; this indicates that the energy barrier for anion complexation does not only result from the dehydration energy of the anion, but also from discriminating host–anion interactions at the transition state. Also note that at a 14 Å distance, there are still important host/anion attractions (about -110 kcal mol^{-1}

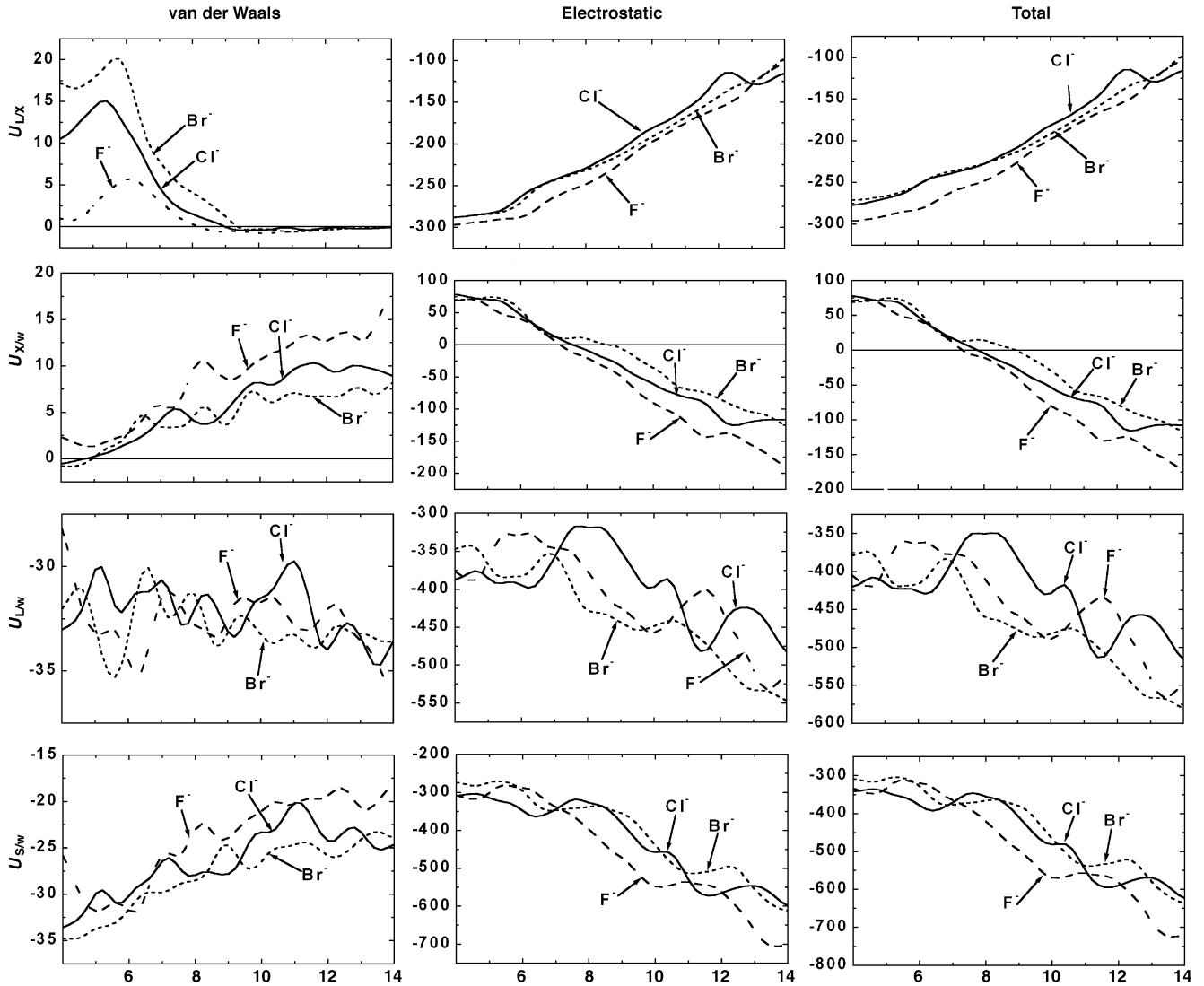

Figure 7. Energy components (van der Waals, electrostatic and total) as a function of the d distance for dissociation of the $X^- \subset \mathbf{L}^{4+}$ complexes in water. Analysis performed on the last configuration (i.e., after 10+10 ps of simulation) at each distance d.

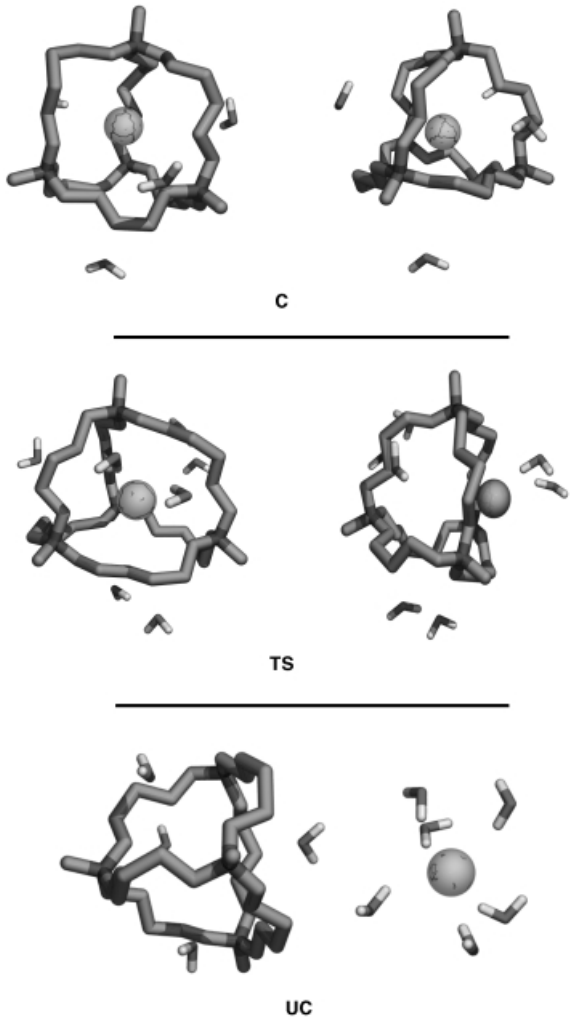

Figure 8. Snapshot of the $Cl^- \subset \mathbf{L}^{4+}$ "complex" in water with selected first shell water molecules: inclusive complex (C), transition state (TS) (orthogonal views) and uncomplexed (UC) state.

for Cl^- and Br^- anions, mainly of electrostatic origin), which are overcompensated by the attraction energies of water with X^- (about $-110\,kcal\,mol^{-1}$) and with $\mathbf{L}^{4+}$ (-492 to $-550\,kcal\,mol^{-1}$). Visual analysis at the graphics system shows that, after the anions exit the cage, their "trajectories" are not linear because no angular constraint was imposed. Comparison of the complexed C and uncomplexed UC states leads to the conclusion that the inclusive complex with F^- is unstable ($\Delta G_{c/uc} = +5.7\,kcal\,mol^{-1}$), while both Cl^- and Br^- complexes are stable $\Delta G_{c/uc} = -7.8$ and $-5.2\,kcal\,mol^{-1}$, respectively). Thus, in water, the $\mathbf{L}^{4+}$ host is predicted to be selective for Cl^- over Br^- by $2.6\,kcal\,mol^{-1}$.

Looking at the deformations of $\mathbf{L}^{4+}$ with respect to its uncomplexed state, one sees that the host is fairly rigid and undergoes only minor structural reorganization and deformations. For instance, upon inclusion of the Br^- anion, its deformation energy ΔU_L changes from 0.0 (uncomplexed state) to $14\,kcal\,mol^{-1}$ (transition state) and $10\,kcal\,mol^{-1}$ (inclusive complex). The corresponding values are 0, 12 and $6\,kcal\,mol^{-1}$ with the Cl^- anion and 0, 9 and $7\,kcal\,mol^{-1}$ with F^-. The structural parameter ρ (Figure 9) is also very similar and changes by about 0.1 unit from the complexed to uncomplexed states and from one anion to the next one. From one inclusive complex to the corresponding transition state, changes in ρ are larger (about 0.4 for Cl^- and Br^-). As expected, the average $\langle NN' \rangle$ distances are similar for the complexed and uncomplexed states, longest near the transition state and shortest for the "facial" anion(s). The surface S of the "gating face" increases at the transition state and follows the order $Br^- > Cl^- > F^-$ (Figure 9).

The conclusions obtained in water from the 15+RF calculations are validated by the 13-PME calculations (see Figure 6 and Table 2). In particular, the F^- complex is predicted to be unstable and to dissociate, while the Cl^- and Br^- complexes are stable. Energy barriers are close and, again, $\mathbf{L}^{4+}$ displays a selectivity for Cl^- over Br^- (by $4.7\,kcal\,mol^{-1}$). The energy difference between the complexed and dissociated states for Cl^- and Br^- is a few $kcal\,mol^{-1}$ smaller with the 15+RF than with the 13-PME protocol. This follows expected trend, as with the former protocol the long range electrostatic interactions are zeroed beyond the cut-off distance, while with the PME they still contribute to the potential energy.

The results of two other methodological variations are reported in Figure 10. The first one corresponds to the F^-, Cl^- and Br^- complexes with reduced sampling (4+6 ps, instead of 10+10 ps) at each step using the TI integration scheme. The second one, performed on the Cl^- decomplexation, uses the FEP method with 10+10 ps of sampling at each window. Comparison with Figure 6 shows that the PMFs are again very similar.

At the end of the PMF simulation (X^- dissociated from $\mathbf{L}^{4+}$), we noticed that the cavity of the host remained empty, that is contained no solvent molecules. This could result from its hydrophobic character, or from insufficient sampling. In order to address this question, we decided to simulate the $H_2O \subset \mathbf{L}^{4+}$ "inclusive complex" where the water molecule was initially placed in the host's cavity. In the gas phase, this

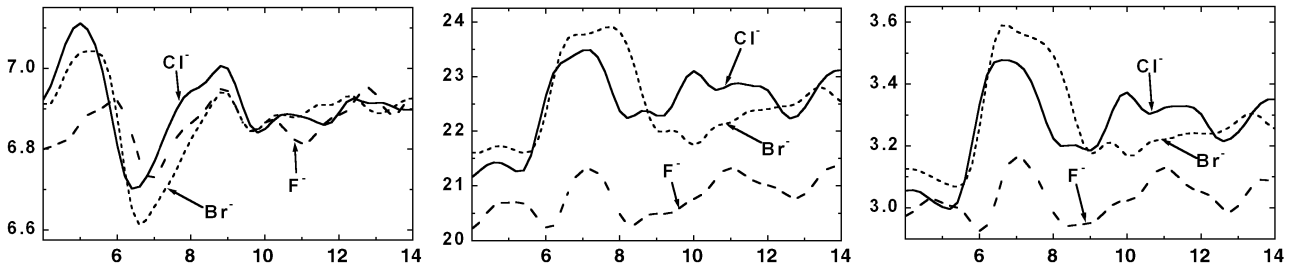

Figure 9. Variation of the average $\langle NN' \rangle$ distances (left), surface S (middle) and the ρ ratio along the dissociation of the F^-, Cl^- and Br^- complexes in water. See text for definitions.

0947-6539/03/0903-0640 $ 20.00+.50/0 *Chem. Eur. J.* **2003**, *9*, No. 3

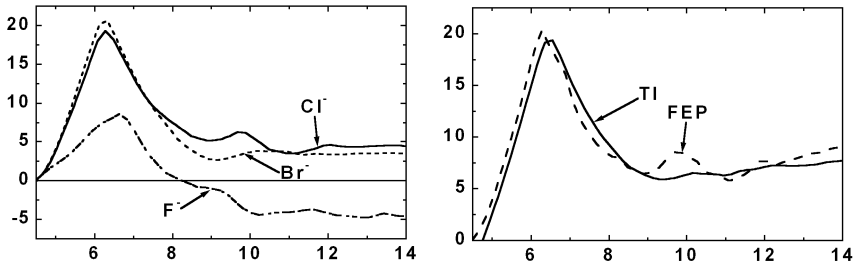

Figure 10. Calculated free energy profiles for the dissociation of $X^- \subset \mathbf{L}^{4+}$complexes in water, using the TI method with 4+6 ps of sampling at each step (left) and PMF of $Cl^- \subset \mathbf{L}^{4+}$complex, with a comparison of TI and FEP methods with 10+10 ps of sampling (right). Calculations performed with a 15+RF cut-off.

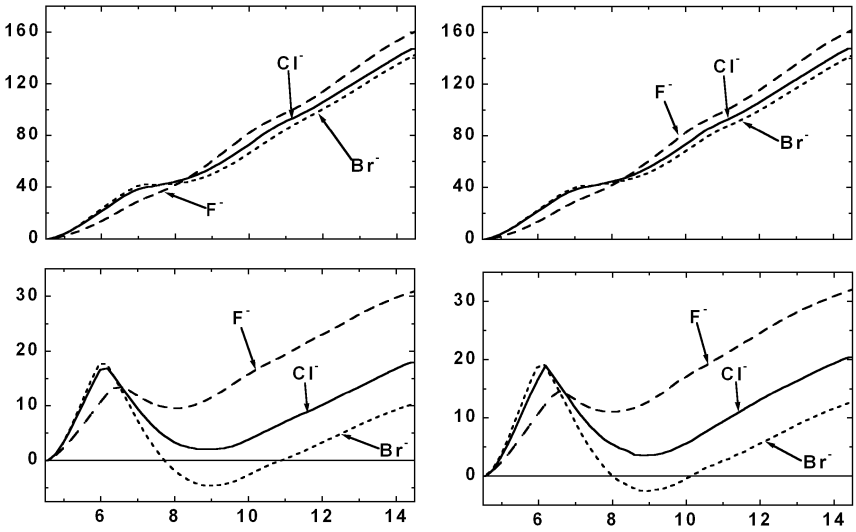

Figure 11. Calculated free energy profiles for the dissociation of $X^- \subset \mathbf{L}^{4+}$complexes in the gas phase with a dielectric constant ε of 1.0 (top) and 5.0 (bottom), using the TI (left) and FEP (right) techniques.

turned out to rapidly decomplex during the dynamics. When the $H_2O \subset \mathbf{L}^{4+}$ complex was immersed and simulated in aqueous solution, the encapsulated water molecule moved from an inclusive to a facial position (enhancing its interaction with $\mathbf{L}^{4+}$ from -2 to -12 kcal mol^{-1}) where it remained for about 0.1 ns, and next diffused to be the bulk aqueous phase, while $\mathbf{L}^{4+}$ underwent some conformational changes, reducing the size of the cavity which became too small to accommodate water molecules as guests. When the dynamics was pushed further up to 3 ns, no water entered into the host's cavity. This clearly demonstrates the hydrophobic nature of this cavity, despite its tetracharged environment.

The conclusions obtained in aqueous solution dramatically differ from those obtained in the gas phase, where the host–guest interactions are mostly of electrostatic origin and dominated by the interactions of the -1 charge of the anion and the positive electrostatic potential created at the center of $\mathbf{L}^{4+}$ by the four ammonium bridgeheads. As a result, the energy $\Delta G(d)$ continuously increases upon dissociation of the complex for the three anions, up to about 150 kcal mol^{-1} at 14 Å for the three anions (Figure 11). The PMF results obtained by the TI technique are also supported by FEP simulations (Figure 11) and contrast with those reported on similar systems by Ichikawa et al. based on MM3 force field calculations.[11] These authors found a marked barrier for the three anions presumably due to an incorrect treatment of electrostatic interactions. The role of electrostatics is indeed demonstrated by repeating the dissociation simulations in the gas phase and using a lower dielectric constant of 5.0 instead of 1.0 (which in fact scales down the coulombic interactions by five). This completely changes the free energy profile and leads to the appearance of a transition state at about 6 Å (i.e., when X^- passes through the [6,6,5] face), followed by an energy minimum at about 8 to 9 Å from F^- to Br^-, which corresponds to "facial complexation". Upon further dissociation, the energy continuously increases, without reaching a plateau, thus following the expected $1/d$ dependence of coulombic interactions with the distance d. Comparison of the end-states for the three anions leads to the conclusion that the F^- complex is the most stable one in the gas phase ($F^- > Cl^- > Br^-$), following the order of host–guest interaction energies. Thus, the comparison of PMFs in the gas phase versus aqueous solution demonstrates the role of solvation on the anion recognition properties of $\mathbf{L}^{4+}$.

Halide anion recognition by $\mathbf{L}^{4+}$ in water—Calculations via the "alchemical route": In this section, we address the question of anion binding selectivity of $\mathbf{L}^{4+}$ in water. As the F^- complex turned out to be unstable and to spontaneously dissociate in water, we restricted the comparison to the Cl^- versus Br^- complexes, which were first equilibrated for 1 ns in the presence of three *exo* Cl^- counterions. The difference in free energies of complexation between Cl^- and Br^- is defined experimentally by $\Delta G_c = \Delta G_1 - \Delta G_2$. It was calculated, based on the following thermodynamics cycle as:

$$\Delta G_c = \Delta G_3 - \Delta G_4,$$

$$\begin{array}{ccc} Cl^-_{aq} + \mathbf{L}^{4+}_{aq} & \xrightarrow{\Delta G_1} & Cl^- \subset \mathbf{L}^{4+}_{aq} \\ {\scriptstyle \Delta G_3}\downarrow & & \downarrow{\scriptstyle \Delta G_4} \\ Br^-_{aq} + \mathbf{L}^{4+}_{aq} & \xrightarrow[\Delta G_2]{} & Br^- \subset \mathbf{L}^{4+}_{aq} \end{array}$$

where ΔG_3 and ΔG_4 correspond to the mutation of Cl^- to Br^-. The calculated difference in free energies of hydration ($\Delta G_3 = 6.3 \pm 0.1$ kcal mol^{-1}) is close to the experimental value of 6.2 kcal mol^{-1}.[15] The ΔG_4 change in free energy for the complexes also increases from the Cl^- to the Br^- complex (by

10.2 ± 0.1 kcal mol^{-1}), thus following the order of host–guest interaction energies. The resulting ΔG_c energy difference indicates that the $\mathbf{L}^{4+}$ host prefers Cl^- over Br^- in aqueous solution, by 3.9 kcal mol^{-1}. This number is very close to the values of 4.7 and 2.6 kcal mol^{-1} reported above from the PMF results of decomplexation.

Discussion and Conclusion

This paper deals with an important theme of supramolecular chemistry, that is molecular recognition of anions,[1–5] which is a feature of biological systems as well. The type of system studied here is particularly interesting, since it concerns the binding of hydrophilic anions by an hydrophobic type receptor, built from quaternary ammonium sites; the anion capture takes place in water, a solvent which strongly competes with the complexation process. To our knowledge, our study is the first one dealing with such systems. There have been FEP simulations on the tetrahedral SC24,4H$^+$ tetraprotonated cryptand with regards to anion recognition, which reproduced the Cl^-/Br^- selectivity, but in this complex the anion is held by strong hydrogen bonds, and no PMF was calculated. Insights into changes in energy components upon Cl^- capture by this host were obtained from MD simulations.[26, 27] Recently, halide anion recognition by an hexaprotonated [*222*,6H$^+$] cryptand in water[28] and the surface activity of anion complexes at liquid/liquid interfaces[29] has been reported. Other simulations dealt with anion complexation through hydrogen bonding in non-aqueous solvents.[30] A review of simulations on anion complexes can be found in reference [31]. Concerning PMF calculations on ion complexation by ionophores, the alkali cation capture and recognition by macrocylic hosts such as valinomycin[32, 33] or 18-[crown]6[34–37] has been reported with several methodologies. Our study is, to our knowledge, the first ones dealing with free energy profiles for anion capture, with a comparison of several anions, and comparison of the binding selectivities derived from different routes. The simulations in explicit solvent, compared with gas phase simulations demonstrate the role of solvation on the capture and recognition of the anion.

We found that the $\mathbf{L}^{4+}$ host does not complex F^-, but does complex Cl^- and Br^- anions in aqueous solution, with a marked selectivity for Cl^-. According to the PMF simulations which follow the decomplexation pathway, the preference $\Delta G_{Cl/Br}$ ranges from 2.6 to 4.7 kcal mol^{-1}, and these numbers are remarkably close to the value of 3.9 kcal mol^{-1} obtained via "alchemical route". The F^- anion, which displays the strongest interactions with $\mathbf{L}^{4+}$ is not complexed in water, because these interactions are not strong enough to compete with the hydration forces. There are, to our knowledge, no stability constants for these complexes in water, but our results are fully consistent with the characterization of the inclusive $Cl^- \subset \mathbf{L}^{4+}$ complex in the solid state[10] and at the interface between a NaCl surface and water,[12] as well as with the preference for Cl^- over Br^- in acetonitrile solution.[11] The tetrahedral analogue of $\mathbf{L}^{4+}$ with four C_5 and two C_6 bridges also binds selectively Cl^-.[11]

From the thermodynamic point of view, complexation results from enthalpic and entropic components, which cannot be directly estimated from the simulations and are unknown from experiment for the studied systems. In the case of macrocylic polyammonium hosts with $>NH_2^+$ binding sites, the anion complexes are of entropic origin,[38, 39] presumably related to the dehydration of the host. Hydrophobic complexation in water is generally also of entropic origin,[40, 41] and it should be emphasized that entropy changes will play an important role for the studied systems. The latter are implicitly accounted for in the MD simulations by the sampling of the configurations along the dissociation pathway. The overall consistency of the results obtained by different routes and methodologies, and agreement with experiment is quite encouraging and suggests that approximations in the force field representation of the system, definition of the "reaction coordinate" and limited separation distance *d* and simulated times are reasonable. They also point to the increasing role of computer simulations in the design of supramolecular architectures for specific recognition properties.[42]

Acknowledgement

The authors are grateful to IDRIS, CINES, Université Louis Pasteur, and PRACTIS for computer resources.

[1] E. Graf, J. M. Lehn, *J. Am. Chem. Soc.* **1976**, *98*, 6403.
[2] J.-M. Lehn, *Supramolecular Chemistry. Concepts and Perspectives*, VCH, Weinheim, **1995**.
[3] J. S. Sessler, J. W. Genge, P. A. Gale, V. Kral in *Calixarenes for Separations* (Eds.: G. J. Lumetta, R. D. Rogers, A. S. Gopalan), ACS, Washington, **2000**, pp. 228.
[4] P. D. Beer, J. Cadman, *Coord. Chem. Rev.* **2000**, *205*, 131.
[5] P. D. Beer, P. A. Gale, *Angew. Chem.* **2001**, *113*, 502; *Angew. Chem. Int. Ed.* **2001**, *40*, 486.
[6] A. Bianchi, K. Bowman-James, E. Garcia-Espana, *Supramolecular Chemistry of Anions,* Wiley-VCH, New York, **1997**.
[7] F. P. Schmidtchen in *Supramolecular Chemistry of Anions* (Eds.: A. Bianchi, K. Bowman-James, E. Garcia-Espana), Wiley-VCH, New York, **1997**, pp. 79.
[8] F. P. Schmidtchen, G. Müller, *J. Chem. Soc. Chem. Commun.* **1984**, 1115.
[9] F. P. Schmidtchen, M. Berger, *Chem. Rev.* **1997**, *97*, 1609.
[10] K. Ichikawa, M. A. Hossain, *Chem. Commun.* **1996**, 1721.
[11] K. Ichikawa, M. Izumi, D. Goto, N. Ito, *Chem. Eur. J.* **2001**, *7*, 5094.
[12] K. Ichikawa, M. Yamada, N. Ito, *Chem. Eur. J.* **1998**, *4*, 914.
[13] N. Ito, M. Izumi, K. Ichikawa, M. Shiro, *Chem. Lett.* **1999**, 1001.
[14] K. Ichikawa, M. A. Hossain, T. Tamura, N. Kamo, *Supramol. Chem.* **1995**, *5*, 219.
[15] Y. Marcus, *Ion Solvation,* Wiley, Chichester, **1985**. Other values have been more reported for absolute free energies of hydration of F^-, Cl^- and Br^-: -105.0, -74.6 and -68.6 kcal mol^{-1} [J. R. Pliego, J. M. Riveros Jr., *Phys. Chem. Chem. Phys.* **2002**, *4*, 1622–1627) and -102.6, -72.7 and -66.5 kcal mol^{-1} (W. R. Fawcett, *J. Phys. Chem. B* **1999**, *103*, 11181–11185), but the differences from one anion to the other are very close.
[16] T. P. Straatsma, J. A. McCammon, *Annu. Rev. Phys. Chem.* **1992**, *43*, 407.
[17] D. A. Case, D. A. Pearlman, J. C. Caldwell, T. E. Cheatham III, W. S. Ross, C. L. Simmerling, T. A. Darden, K. M. Merz, R. V. Stanton, A. L. Cheng, J. J. Vincent, M. Crowley, D. M. Ferguson, R. J. Radmer, G. L. Seibel, U. C. Singh, P. K. Weiner, P. A. Kollman, *AMBER5*, University of California, San Francisco, **1997**.

  0947-6539/03/0903-0642 $ 20.00+.50/0

[18] W. L. Jorgensen, J. Chandrasekhar, J. D. Madura, *J. Chem. Phys.* **1983**, *79*, 926.
[19] F. Berny, *PhD Thesis*, Université Louis Pasteur, Strasbourg, **2000**.
[20] T. P. Lybrand, I. Ghosh, J. A. McCammon, *J. Am. Chem. Soc.* **1985**, *107*, 7793.
[21] I. G. Tironi, R. Sperb, P. E. Smith, W. F. van Gunsteren, *J. Chem. Phys.* **1995**, *102*, 5451.
[22] H. J. C. Berendsen, J. P. M. Postma, W. F. van Gunsteren, A. DiNola, *J. Chem. Phys.* **1984**, *81*, 3684.
[23] M. P. Allen, D. J. Tildesley, *Computer Simulation of Liquids* (Eds.: W. F. van Gunsteren, P. K. Weiner), Clarendon, Oxford, **1987**.
[24] P. Kollman, *Chem. Rev.* **1993**, *93*, 2395.
[25] Only with F^- as anion, there is a small peak, corresponding to 0.2 H_2O molecules, in keeping with the poor shielding of this anion by the cage.
[26] B. Owenson, R. D. MacElroy, A. Pohorille, *J. Am. Chem. Soc.* **1988**, *110*, 6992.
[27] B. Owenson, R. D. MacElroy, A. Pohorille, *THEOCHEM* **1988**, *179*, 467.
[28] P. Jost, R. Schurhammer, G. Wipff, *Chem. Eur. J.* **2000**, *23*, 4255.
[29] A. Chaumont, G. Wipff, *J. Comput. Chem.* **2002**, *23*, 1532.
[30] N. A. McDonald, E. M. Duffy, W. L. Jorgensen, *J. Am. Chem. Soc.* **1998**, *120*, 5104.
[31] J. Wiorkiewicz-Kuczera, K. Bowman-James in *Supramolecular Chemistry of Anions* (Eds.: A. Bianchi, K. Bowman-James, E. Gracia-Espana), Wiley-VCH, New York, **1997**, pp. 335.
[32] T. J. Marrone, J. K. M. Merz, *J. Am. Chem. Soc.* **1992**, *114*, 7542.
[33] T. J. Marrone, K. M. Merz, *J. Am. Chem. Soc.* **1995**, *117*, 779.
[34] L. X. Dang, P. A. Kollman, *J. Am. Chem. Soc.* **1990**, *112*, 5716.
[35] L. X. Dang, P. A. Kollman, *J. Phys. Chem.* **1995**, *99*, 55.
[36] J. van Eerden, W. J. Briels, S. Harkema, D. Feil, *Chem. Phys. Lett.* **1989**, *164*, 370.
[37] T. J. Marrone, D. S. Hartsough, K. M. Merz, *J. Phys. Chem.* **1994**, *98*, 1341.
[38] J. Cullinane, R. I. Gelb, T. N. Margulis, L. J. Zompa, *J. Am. Chem. Soc.* **1982**, *104*, 3048.
[39] R. I. Gelb, B. T. Lee, L. J. Zompa, *J. Am. Chem. Soc.* **1985**, *107*, 909.
[40] W. Blokzijl, J. B. F. N. Engberts, *Angew. Chem.* **1993**, *105*, 1610; *Angew. Chem. Int. Ed. Engl.* **1993**, *32*, 1545.
[41] D. B. Smithrud, F. Diederich, *J. Am. Chem. Soc.* **1990**, *112*, 339.
[42] *Computational Approaches in Supramolecular Chemistry*, NATO ASI (Ed.: G. Wipff), Kluwer, Dordrecht, **1994**.

Received: August 23, 2002 [F4368]